Behavioural Brain Research 320 (2017) 233–243

Contents lists available at ScienceDirect

Behavioural Brain Research

journal homepage: www.elsevier.com/locate/bbr

Research report

Mental rotation task specifically modulates functional connectivity strength of intrinsic brain activity in low frequency domains: A maximum uncertainty linear discriminant analysis

Mengxia Gao[a,1], Delong Zhang[a,1], Zengjian Wang[a], Bishan Liang[b], Yuxuan Cai[a], Zhenni Gao[a], Junchao Li[a], Song Chang[a], Bingqing Jiao[a], Ruiwang Huang[a,*], Ming Liu[a,*]

[a] Center for the Study of Applied Psychology, Key Laboratory of Mental Health and Cognitive Science of Guangdong Province, School of Psychology, South China Normal University, Guangzhou, China
[b] College of Education, Guangdong Polytechnic Normal University, China

HIGHLIGHTS

- MLDA method effectively discriminates the resting and task state based on FCS.
- The modulation of FCS is observed in the low frequency band 0.05–0.1 Hz.
- Imagery-based and executive-control function are differently involved in mental rotation.
- Exploration of modulation effect provides full view of the neural basis of mental rotation.

ARTICLE INFO

Article history:
Received 1 November 2016
Received in revised form
12 December 2016
Accepted 15 December 2016
Available online 20 December 2016

Keywords:
Mental rotation task
Resting-state fMRI
Discriminant analysis
Voxel-wise functional connectivity strength
Frequency-bandwidth

ABSTRACT

Neuroimaging studies have highlighted that intrinsic brain activity is modified to implement task demands. However, the relation between mental rotation and intrinsic brain activity remains unclear. To answer this question, we collected functional MRI (fMRI) data from 30 healthy participants in two mental rotation task periods (1st-task state, 2nd-task state) and two rest periods before (pre-task resting state) and after the task (post-task resting state) respectively. By combining the spatial independent component analysis (ICA) and voxel-wise functional connectivity strength (FCS), we identified FCS maps of 10 brain resting state networks (RSNs) within six different bands (i.e., 0–0.05, 0.05–0.1, 0.1–0.15, 0.15–0.2, 0.2–0.25, and 0.01–0.08 Hz) corresponding to the four states for each subject. The maximum uncertainty linear discriminant analysis (MLDA) method showed that the FCS within the low frequency bandwidth of 0.05–0.1 Hz could effectively classify the mental rotation task state from pre-/post-task resting states but failed to discriminate the pre- and post-task resting states. Discriminative FCSs were observed in the cognitive executive-control network (central executive and attention) and the imagery-based internal mental manipulation network (default mode, primary sensorimotor, and primary visual). Imagery manipulation is a stable mental element of mental rotation, and the involvement of executive control is dependent on the degree of task familiarity. Together, the present study provides evidence that mental rotation task specifically modifies intrinsic brain activity to complement cognitive demands, which provides further insight into the neural basis of mental rotation manipulation.

© 2016 Elsevier B.V. All rights reserved.

1. Introduction

Recent functional imaging studies have shown that intrinsic brain activity is the baseline of cognition processes, in which resting-state brain activity is modified to implement cognition demands [1,2]. The modification of intrinsic brain activity is depending on the task demand, such as the goal-directed task [3] and the internally directed tasks [4,5]. In particular, the mental

* Corresponding authors at: Center for the Study of Applied Psychology, Key Laboratory of Mental Health and Cognitive Science of Guangdong Province, School of Psychology, South China Normal University, Guangzhou 510631, China.
E-mail addresses: ruiwang.huang@gmail.com (R. Huang), lium@scnu.edu.cn (M. Liu).
[1] These authors contributed equally to this work.

http://dx.doi.org/10.1016/j.bbr.2016.12.017
0166-4328/© 2016 Elsevier B.V. All rights reserved.

rotation task in which participants make a decision about orientating visual images by manipulation during mental imagining [6], is not only a classical "internally directed" task [7] but also embodies goal-directed attributes [8]. However, the linkage between the mental rotation state and intrinsic brain activity still remains largely unclear.

It is well established that intrinsic brain activity is self-organized into a spatial structure [9] and the evoked neural responses to tasks are embedded in this functional architecture [10]. First, intrinsic brain activity has been observed to be highly trait-related, in which many studies have shown that it is significantly modified by many traits, such as brain disease [11–13], intelligence [14], personality [15], age [16], and gender [17]. At the same time, intrinsic brain activity exhibits dynamically adaptive reconfiguration during active task performance [18]. Recently, many studies have showed the existence of the modulation effect on intrinsic brain activity from task engagements, including simple visual tasks [19–21], auditory task [22], attention task [23], memory task [24], and motor learning task [25]. Of note, most of the modulatory effects on intrinsic brain activity from different cognitive tasks were found in the low-frequency bandwidth (0.01–0.1 Hz) [1,26–28]. Although the significant modulation effect of task demands on intrinsic brain activity has been widely reported, distinct task demands have been rarely studied, which may induce different modifications. Particularly, many studies found that the default mode network (DMN) was deactivated during some externally goal-directed tasks [29–31]. In contrast to these observations, it was recently found that the involvement of internal processing cognition task could cause activation of the DMN [4,5], and during the maintenance period of a working memory task, brief task-unrelated visual stimuli increased the activity of the DMN [32].

As a specific task demand, the mental rotation task allows one to judge an object's orientation in their mind and was first proposed by Shepard and Metzler [6]. The completion of an mental rotation task requires at least 5 cognitive steps [33]: (I) visually perceiving and encoding the presented object, (II) imagining the object and its orientation, (III) rotating the object mentally, (IV) making a judgment whether the object is similar to the target object, and (V) making the final decision. Regarding the behavior response aspect, it has been widely proven that the reaction time (RT) required to make a judgment always increases in a near-linear fashion with increasing numbers of angles [8,34,35]. To explore the neural substrates of mental rotation, neuroimaging studies have identified many brain regions responding to mental rotation task [8], in which the prefrontal and parietal cortex have been suggested to be highly associated with mental rotation task demands [36–40]. The activation of prefrontal regions is thought to be involved in comparing the target object with the mentally rotated object [41], whereas the parietal cortex is thought to participant in mediating visual and somatosensory input message and generating of rotated movements in the visual space [42]. More specifically, the secondary motor areas (i.e., the premotor cortex and supplementary motor area) are thought to be involved in computing rotation angles, matching objects and making the final decision [43]. These observations provide evidence for the complex mental components involved in mental rotation task and shed light upon the neural basis that underlies mental rotation perception process. However, few studies have focused on the neural response of the intrinsic brain activity modified by mental rotation task.

To fill this gap, the present study aimed to explore the changes of the functional connection architecture of intrinsic brain activity in the pre-/post-task resting states and mental rotation task state and investigate the modulation effect of the specific task on resting-state brain activity. To this end, we collected fMRI data from 30 healthy subjects during four states: a pre-task resting state, two mental rotation states (1st-task state and 2nd-task state), and a post-task resting state. Then, we estimated the voxel-wise functional connectivity strength (FCS) based on a graph theoretical method [44,45] related to different frequency bands (i.e., 0–0.05 Hz, 0.05–0.1 Hz, 0.1–0.15 Hz, 0.15–0.2 Hz, 0.2–0.25 Hz, and 0.01–0.08 Hz) [46] to measure the brain functional connection architecture. To further depict the details of the brain connections, we performed a spatial independent component analysis (ICA) to identify the resting-state networks (RSNs) and to further calculate the FCS maps of these RSNs. Meanwhile, a pattern recognition method, a maximum uncertainty linear discriminant analysis (MLDA) [47–49], was applied to detect the changes in the FCS of these RSNs within each frequency band between any two of the four states. Finally, we validated the findings of the present study using an anatomical automatic labeling (AAL) atlas [50].

2. Materials and methods

2.1. Participants

Thirty right-handed, healthy participants (15 males, age 19–25 years) were recruited from the South China Normal University (SCNU) for the present study. All participants had normal or corrected-to-normal vision. None had a history of neurological or psychiatric disorders according to their self-reports. The protocol was approved by the Research Review Board of SCNU. Written informed consent was obtained from each participant.

2.2. Experiment stimuli

In the present study, the letter "R" was selected from the rotation-arrow task devised by Shah and Miyake [51] and was used in the mental rotation task. The stimuli were presented as normal or as mirror-image in 4 orientations: (1) 0°, (2) 45°, (3) 90°, and (4) 135° (Fig. 1).

2.3. Behavioral task and procedure

Fig. 2 shows the stimuli and the procedure of the mental rotation task which corresponded to a previous study [51]. Briefly, the present study contained 4 experimental conditions (i.e., 0°, 45°, 90°, and 135°), which were presented using an event-related design with 2 parts. A total of 128 trials were presented randomly per part (80 trials in the 1 st task and 48 trials in the 2nd task). A rest period of approximately 2 min was allowed between the 2 parts to prevent fatigue. For each trial, a fixation point (500 ms) was first presented, followed by a first letter (normal-R or mirror-R, 1000 ms), then a mask (5000 ms), and finally a second letter (rotated normal-R or mirror-R). The participants were asked to decide whether the second letter was the same to the first letter (normal or mirror) by pressing a button within 5000 ms using the right thumb to indicate the same and the left thumb to indicate a difference. Stimuli were presented using *E*-prime software (http://www.e-prime.pl). Before fMRI scanning, participants performed practice sessions until they reached an accuracy of 90% outside the scanner.

There were a total of three scans during the MRI scanning. During the first and third scans, we acquired resting-state fMRI (R-fMRI) data for 8 min. The participants were instructed to lie quietly with their eyes fixed at the black fixation cross on the screen. During the second scan, we obtained the task-state fMRI (T-fMRI) data while the participants performed the mental rotation task.

A median absolute deviation estimator [52] based on the correct response time (RT) was applied to eliminate outlier trials, and the average RTs of the correct responses were subsequently calculated for each participant. A one-way ANOVA with a rotation angle

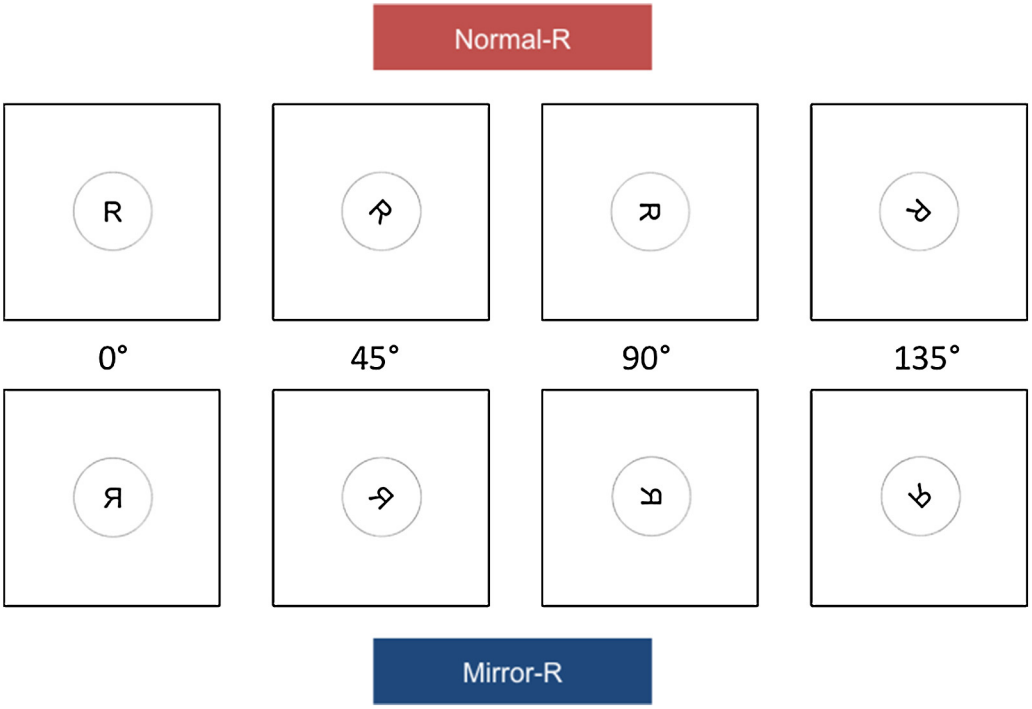

Fig. 1. Samples of rotated stimuli of the mental rotation task.

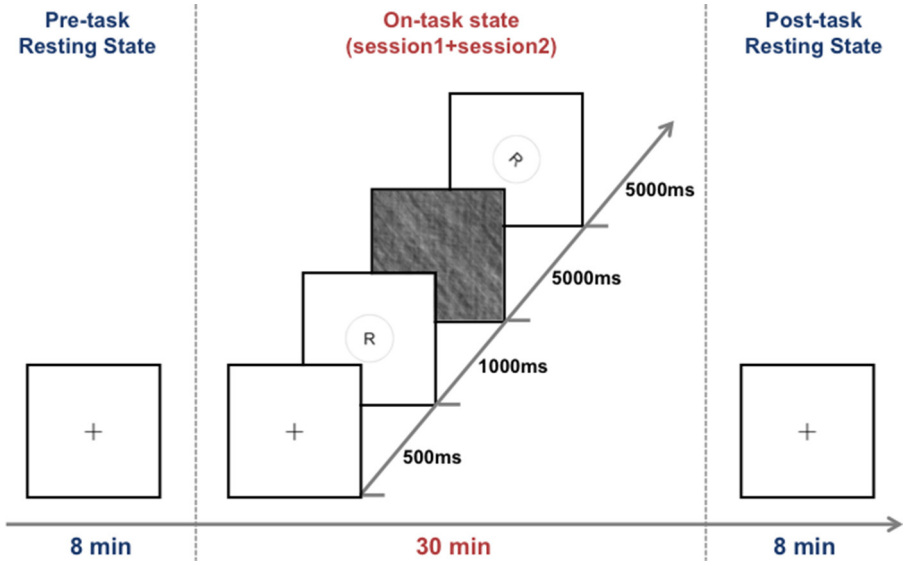

Fig. 2. Illustration of the experimental procedure.

(i.e., 0°, 45°, 90°, and 135°) as the within-subject variable was then applied to the average RTs.

2.4. MRI data acquisition

We acquired all MRI data using a 3T Siemens Trio Tim MR scanner with a twelve-channel phased-array head coil at the Brain Imaging Center at SCNU. Functional images were obtained by using a GE-EPI sequence (TR/TE/Flip Angle = 2000 ms/30 ms/90°, FOV = 220 mm, matrix = 64 × 64, thickness/gap = 3.5/0.8 mm, 32 axial interleaved slices, and 240 vol). In addition, we used a T1-weighted 3D MP-RAGE sequence to obtain high resolution brain structural images for each participant (TR/TE/Flip Angle = 1900 ms/2.52 ms/9°, FOV = 100 mm, matrix = 256 × 256, thickness = 1 mm, pixel bandwidth = 170, and 176 vol). The total scanning time was approximately 55 min for each participant.

2.5. Image pre-processing

The images of the pre-task, mental rotation task (1st-task and 2nd-task), and post-task states were preprocessed using SPM8 (http://www.fil.ion.ucl.ac.uk/spm/). The first 10 functional volumes were discarded to allow for saturation effects of the BOLD signal and adaptation of the participants to the scanning environment. Then, the remaining fMRI images underwent slice timing and head motion correction. Two datasets (one of the pre-task state and the other of the post-task state) were excluded due to excessive head motion based on the criteria, translation < 3 mm and rotation < 3°

[53]. The corrected volumes were then spatially normalized to the standard Montreal Neurological Institute (MNI) space using an optimum 12-parameter affine transformation and nonlinear deformation [54]. The resulting data were further temporally band-pass filtered into a conventional frequency band of 0.01–0.08 Hz. In addition, we also divided the full frequency range (0–0.25 Hz) into five different bands (i.e., 0–0.05, 0.05–0.1, 0.1–0.15, 0.15–0.2, and 0.2–0.25 Hz) [46] to detect the changes between different states in the low- and high-frequency domains.

2.6. Voxel-wise functional connectivity strength (FCS)

The voxel-wise FCS has been widely used to reflect the connection characteristics of large-scale RSNs, which is based on a data-driven graph theoretical method to measure the functional hubs of RSNs [44,45]. To calculate the FCS, Pearson correlation coefficients were computed between the time courses of voxels (number = n) of the brain within the gray matter (GM) mask [55]. The GM mask was adopted from the default brain mask of the Resting state fMRI Data Analysis Toolkit (Rest, http://rest.restfmri.net), and an $n \times n$ matrix between any pair of voxels was then yielded. Subsequently, the matrices of all the participants were further transformed into a z-score matrix using Fisher's r-to-z approach within each participant and further smoothed with a Gaussian kernel of 6 mm full-width at half-maximum. The sum of the connections for a given voxel and all other voxels indicates its central roles in transferring information across RSNs. Such a FCS metric is also referred to as the "degree centrality" of weighted networks in terms of graph theory. All FCS calculations were completed using the Rest toolkit.

2.7. Group spatial ICA

We adopted a group spatial ICA analysis (GIFT, http://icatb.sourceforge.net) on the data from all participants to identify the RSNs of intrinsic brain activity [56]. Each BOLD time series except for the first 5 vol was motion-corrected, normalized to the standard Montreal Neurological Institute (MNI) space [54] and resampled to a voxel size of $3 \times 3 \times 3$ mm^3 using SPM8 (http://www.fil.ion.ucl.ac.uk/spm/). The group independent component analysis (Group ICA) was based on the data of the pre-processed resting state and the first 235 vol of the mental rotation task state for all participants. The group ICA included a two-stage principal component analysis (PCA) reduction [57], ICA separation, and back-reconstruction to produce single-subject time courses and spatial maps [57]. The optimal number of ICs was estimated as 38 based on the minimum description length (MDL) criteria, and the data were separated by ICA using the Informax algorithm [58]. This step generated a spatial map and a time course of the BOLD signal changes for each IC. This analysis was repeated 20 times using ICASSO to assess the repeatability [59]. Then, the IC time courses and spatial maps were used for the back-reconstruction procedure for each participant [57,60].

To define RSNs, we converted the spatial maps of each IC into z-scores and entered the averaged maps into a one-sample t-test (false discovery rate, FDR corrected, $p < 0.00001$). For each IC spatial map, a group level t-map was generated, and the t-map was used to define the RSNs. Finally, we identified 10 RSNs in the present study.

2.8. Statistical analysis

To determine the effects of the frequency band on the FCS, we performed a one-way analysis of variance (ANOVA) with states (pre-task, mental rotation task and post-task states) as a factor for each of the 6 frequency bandwidths. All the results were corrected for multiple comparisons to a significant level of $p < 0.05$ with cluster size > 85 voxels based on false discovery rate (FDR) correction [61]. Based on this result, an optimized frequency bandwidth was finally selected.

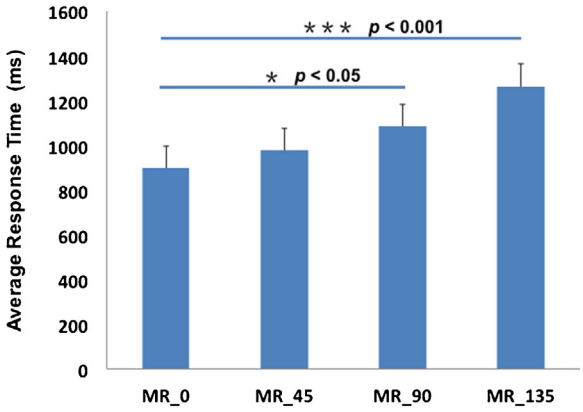

Fig. 3. RTs of the mental rotation task for the 4 conditions.

2.9. Discriminative analysis

This study applied the MLDA-based classification method [62] to classify any two of the four states (pre-task state, 1st-task state, 2nd-task state, and post-task state). As we know, the primary idea of LDA is to transform multivariate observed values to univariate values, maximize the between-class separation and minimize the within-class variance ratio. Thomaz et al. renamed this method as the "MLDA", which employed the maximum entropy covariance selection method to stabilize the within-class scatter matrix with a multiple of the identity matrix [62]. In this study, we extracted the mean FCSs of each RSN from the spatial IC map of each participant, and the mean FCSs of each network were used as the features for the discriminative analysis. A feature selection procedure was performed on the training sample, in which two-sample t tests were carried out to determine the features that showed significant between-state differences ($p < 0.05$). Then, the leave-one-out cross validation (LOOCV) approach was employed to validate the performance of the discriminative classifier. For details, we selected one subject as a test sample and used the remaining $n - 1$ subjects to build a multi-classifier for n (n indicates the total number of subjects) times. Feature selection was restricted only in the training dataset to maintain independence of the training and testing data. After this step, each base classifier's voting weight was obtained by calculating the classification accuracy of $n - 1$ leave-one-out within the training set. Higher feature weights of the voting corresponded to more discriminative features. Finally, we acquired the total contribution of the feature (FCS) to the classification of the 10 RSNs.

2.10. Validation analysis

In this study, we validated whether the main findings of the present study could be repeated by using other feature extraction approaches. To this end, the individual FCS maps were further divided into 90 regions of interest (ROIs) by applying the automated anatomical labeling (AAL) atlas [50], and the data analysis based on the 10 RSNs was repeated using the data related to the AAL atlas.

3. Results

3.1. Behavior performance

All participants performed well (accuracy is above 89.1%) except one (approximately 76%) in all the conditions. The ANOVA revealed

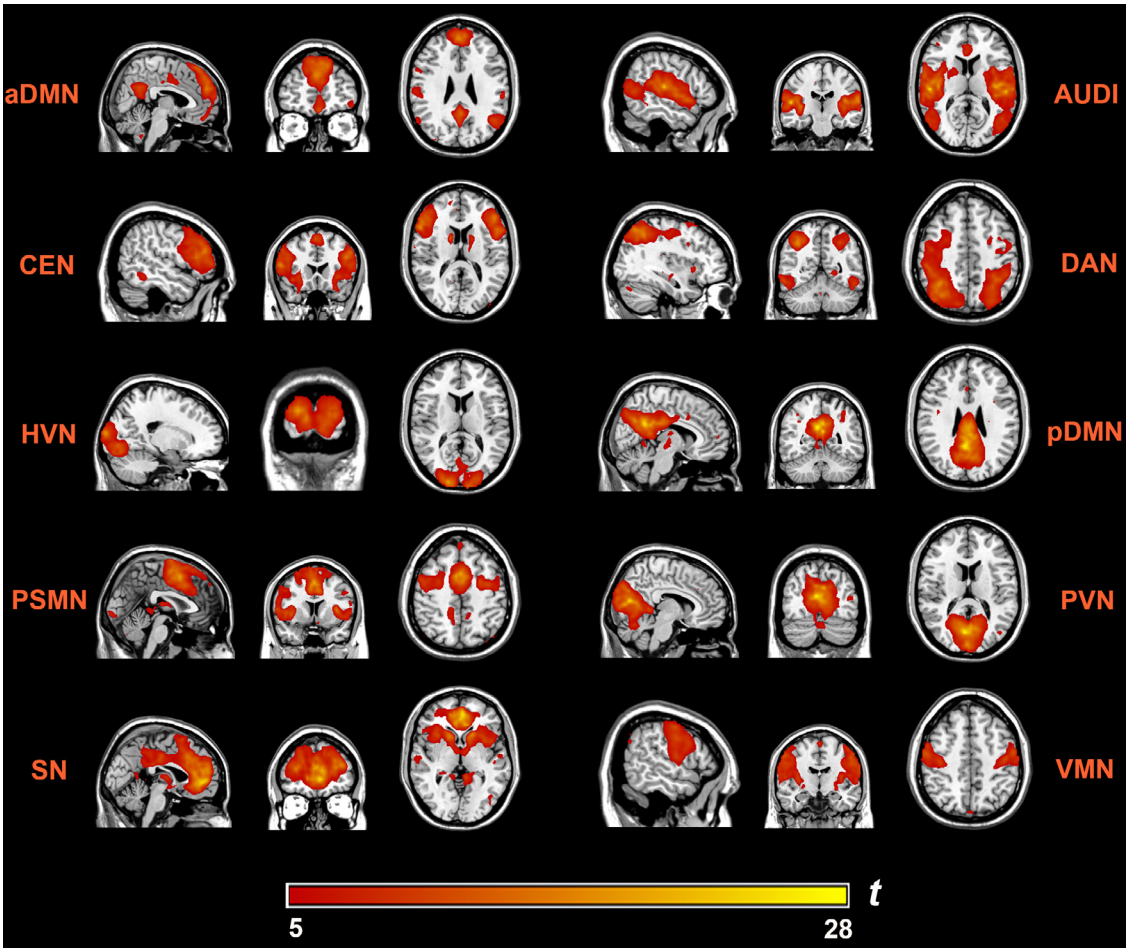

Fig. 4. The 10 RSNs identified from the spatial IC maps. aDMN, anterior part of the default mode network; AUDI, auditory network; CEN, central executive network; DAN, dorsal attention network; HVN, high-order visual network; pDMN, posterior part of the default mode network; PSMN, primary sensory motor network; PVN, primary visual network; SN, salience network; and VMN, ventro-lateral motor network. Each brain map is the result of a one-sample *t* test on the averaged individual map ($p < 0.00001$, FDR corrected).

that there was a significant difference in RTs among the 4 mental rotation (MR) conditions (MR_0, MR_45, MR_90, and MR_135) ($F(3, 116) = 13.18$, $p < 0.001$). Pairwise post-hoc analysis using Tukey HSD revealed that the significant differences occurred between the MR_135 condition and all the other conditions ($p < 0.001$ in the MR_0 vs. MR_135, $p < 0.001$ in the MR_45 vs. MR_*135*, $p < 0.05$ in the MR_90 vs. MR_*135*) and a significant difference between the MR_0 condition and the MR_90 condition ($p < 0.05$) (see Fig. 3). Nevertheless, there was a salient trend that greater rotation angles corresponded to higher RTs required to complete the mental rotation task, which corresponded to the premises.

3.2. Resting-state networks identification

By using the group ICA method, this study identified 10 RSNs: the anterior part of the default mode network (aDMN) (e.g., the superior and medial frontal gyrus), the auditory network (AUDI) (e.g., the bilateral superior temporal gyrus), the central executive network (CEN) (e.g., the bilateral inferior frontal gyrus, the middle frontal gyrus and the precentral gyrus), the dorsal attention network (DAN) (e.g., the superior and inferior parietal regions), the high-order visual network (HVN) (e.g., the middle occipital gyrus), the posterior part of the default mode network (pDMN) (e.g., the precuneus regions and the posterior cingulate cortex), the primary sensory motor network (PSMN) (e.g., the supplementary motor area), the primary visual network (PVN) (e.g., the calcarine and lingual regions), the salience network (SN) (e.g., the anterior cingulate regions, the superior and medial frontal gyrus, and the insula regions), and the ventro-lateral motor network (VMN) (e.g., the postcentral gyrus). According to prior studies, RSNs, such as the AUDI, HVN, PSMN, PVN and VMN, belong to lower-level sensory processing, while the aDMN, CEN, DAN and pDMN are associated with higher-order cognitive processing [63–65]. Table 1 and Fig. 4 show the detailed information and spatial maps of these 10 RSNs. These identified RSNs highly matched those previously reported [65–67].

3.3. Group-level statistical analysis results for FCS

Among the 6 frequency bandwidths, one-way ANOVA showed that the most significant differences in FCS were observed in the 0.05–0.1 Hz band (Fig. 5). The main effects were identified in the bilateral insula, the right middle cingulum, the left inferior occipital gyrus, the left inferior parietal gyrus, the right medial part of the superior frontal gyrus, the right inferior temporal gyrus, the right angular gyrus, the left middle occipital gyrus, the bilateral superior frontal gyrus and the right cerebellum 6. Based on these results, the band of 0.05–0.1 Hz was chosen as the optimal band and was used in the following calculations. The results of the other frequency bandwidths are shown in the Supplementary materials (Fig. S1).

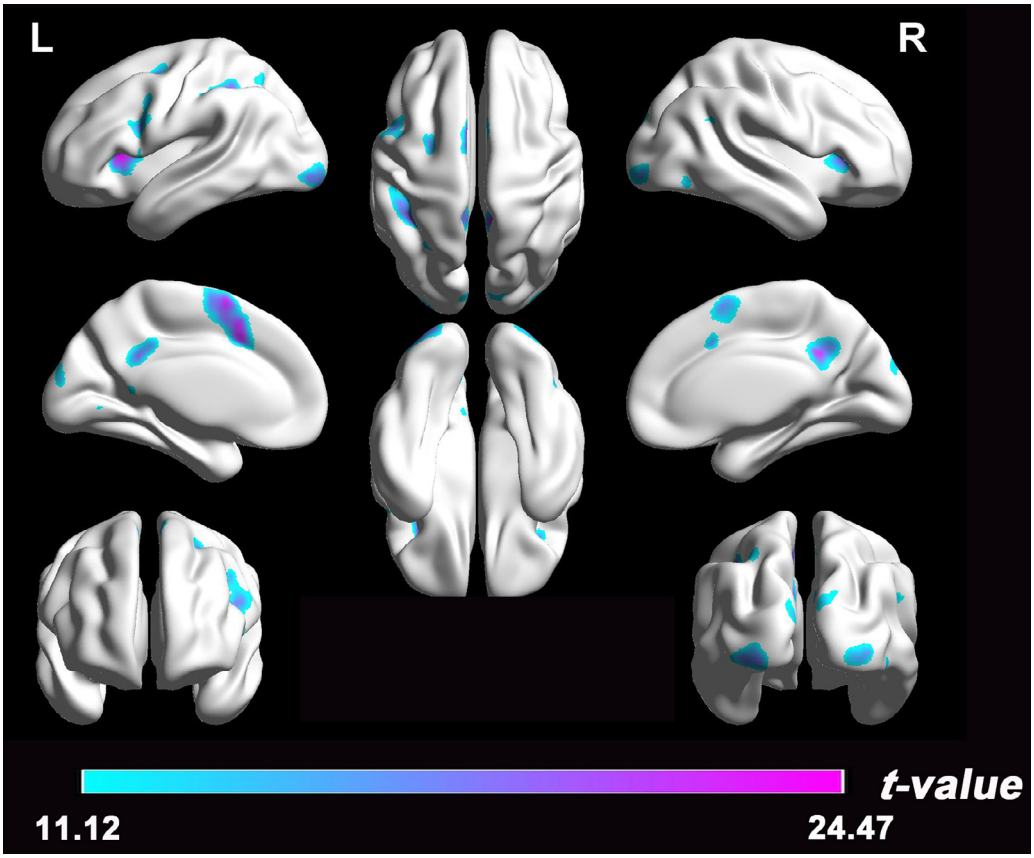

Fig. 5. The surface representation of the main effects on FCS within the band of 0.05–0.1 Hz. The colorbar indicates the *t* value. The 3D maps were generated using the BrainNet Viewer (http://www.nitrc.org/projects/bnv/). L (R), left (right) hemisphere.

Table 1
Details of the selected 10 RSNs.

Index	RSNs	Regions	MNI Coordinates			*t*-value
			x	*y*	*z*	
1	aDMN	Frontal_Sup_Medial_R	3	51	27	17.14
2	AUDI	Temporal_Sup_R	54	−21	12	27.05
3	CEN	Frontal_Inf_Tri_L	−45	33	12	19.08
4	DAN	Parietal_Inf_R	36	−54	48	18.16
5	HVN	Cuneus_R	18	−99	12	19.53
6	pDMN	Precuneus_R	6	−51	27	27.6
7	PSMN	Supp_Motor_Area_L	0	9	51	20.62
8	PVN	Calcarine_R	6	−75	15	27.69
9	SN	Cingulum_Ant_L	−3	48	0	26.18
10	VMN	Postcentral_L	−42	−15	45	13.29

The 10 RSNs are the same as those in Fig. 4. The coordinates of the peak voxel for each RSN are presented in the MNI space. The regions where the peak voxels are located, are reported according to the AAL atlas, as follows: Frontal_Sup_Medial_R, the right superior frontal gyrus, medial; Temporal_Sup_R, the right superior temporal gyrus; Frontal_Inf_Tri_L, the left inferior frontal gyrus, triangular part; Parietal_Inf_R, the right inferior parietal, including supramarginal and angular gyri; Cuneus_R, the right cuneus; Precuneus_R, the right precuneus; Supp_Motor_Area_L, the left supplementary motor area; Calcarine_R, the right calcarine fissure and surrounding cortex; Cingulum_Ant_L, the left anterior cingulum; and Postcentral_L, the left postcentral gyrus. The *t* value indicates the results of one-sample *t*-test on the individual IC pattern ($p < 0.00001$, FDR corrected).

Table 2
Classification results of the FCS related to 10 RSNs and 90 ROIs.

Conditions	10 RSNs			90 ROIs		
	Sensitivity	Specificity	Accuracy	Sensitivity	Specificity	Accuracy
Pre-task vs. 1st-task	**89.66%**	**73.33%**	**81.36%**	**93.10%**	**80.00%**	**86.44%**
Pre-task vs. 2nd-task	**79.31%**	**70.00%**	**74.58%**	**82.76%**	**60.00%**	**71.19%**
1st-task vs. 2nd-task	53.33%	60.00%	56.67%	70.00%	63.33%	66.67%
1st-task vs. post-task	**93.10%**	**83.33%**	**88.14%**	**89.66%**	**86.67%**	**88.14%**
2nd-task vs. post-task	62.07%	70.00%	66.10%	65.52%	66.67%	66.10%
Pre-task vs. Post-task	–	–	–	44.83%	55.17%	50.00%

Bold font indicates that the classification accuracy is higher than 70%.

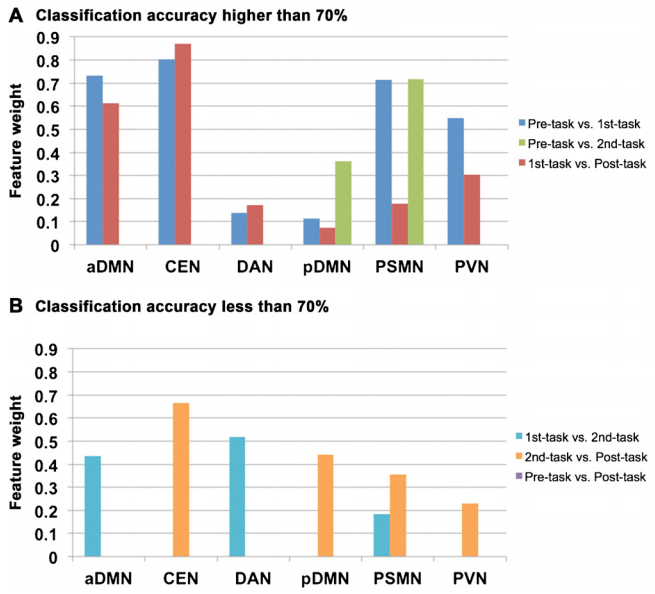

Fig. 6. The contributive features of FCS for classification with discriminative power related to 10 RSNs. (A) Contributive features for classification accuracy higher than 70%. (B) Contributive features for classification accuracy less than 70%.

3.4. Classification results of the 10 resting state networks

By using the mean FCSs of the identified 10 RSNs as features, we found that the MLDA method could effectively classify the task and resting states. Focusing on the 1st-task state, we found that the classification accuracy between the 1st-task state and the pre-task resting state was 81.36% and between the 1st-task state and the post-task resting state the accuracy was 88.14%. With respect to the 2nd-task state, we found that the FCS achieved a classification accuracy of 74.58% between the 2nd-task state and the pre-task resting state, and the accuracy was less than 70% between the 2nd-task state and the post-task resting state. The classification accuracy between the two task states was less than 70%. Moreover, there was no significant difference between the pre-task and post-task resting states, which meant there was no feature that was selected according to the current criterion in the feature selection step (Table 2).

Further analyses showed that the selected RSNs yielded different contributions in classifying the two task states from the pre-task resting state. The RSNs, including the CEN, aDMN, PSMN, PVN, DAN, and pDMN, had a relatively high classification power for differentiating the pre-task resting state from the 1st-task state, while the PSMN and pDMN performed well in identifying the pre-task resting state from the 2nd-task state. Of note, the selected features with discriminative power were distinct in the classification of the pre-task resting state from the two task states. Moreover, we noted that, the higher cognitive networks (CEN and aDMN) rather than the lower sensory networks (PSMN and PVN) had greater power for classifying the 1st-task state from the pre-task resting state. However, to classify the 2nd-task state from the pre-task resting state, the lower sensory networks had greater power. We did not find any features in discriminating the pre-task and the post-task resting states, and we observed that the contributed features for classifying the two task states from the post-task resting state were the same as those which classified the two task states from the pre-task resting state, in which the cognitive networks and sensory networks were both involved in classification. The discriminative features and their contributions on classification are shown in Fig. 6.

3.5. Validation results

By using the AAL atlas, we extracted the FCS map of the whole brain and further repeated the classification analysis between the resting states and the task states. We found that the main findings using the 10 RSNs were also observed based on the AAL maps. The classification performance of the FCS is shown in Table 2, and the discriminative features are shown in Fig. 7. Particularly, the top 15 features shown in different colors are listed in descending order of their weights. Different colors indicate different brain functional networks according to a former study [68].

4. Discussion

In the present study, we applied the MLDA method to investigate the classification among resting state and task state to further explore the relation between mental rotation and intrinsic brain activity. The main findings can be summarized as follows: (1) the most significant FCS change between the resting states and the mental rotation task states was observed in the low frequency bandwidth (0.05–0.1 Hz), and the MLDA method was effective in identifying the alteration between different states based on FCS; (2) the most discriminative features for differentiating the states were the CEN, aDMN, PSMN, PVN, pDMN and DAN, many of which are involved in the cognitive process of mental rotation; (3) the discriminative patterns required to classify the pre-task resting state, the post-task resting state, and the two mental rotation task states were quite different, which shows the specific modification of mental rotation on intrinsic brain activity.

Based on graph theory, FCS is an unbiased method for characterizing the functional network of the entire brain in rest and during a task state [55,69–71]. Notably, FCS approaches have been adopted to investigate the relationship between resting and working-memory task states [44], the topology of the DMN in predicting attention task performance [72], and positive and negative affective processing during picture-viewing task [73]. Applying FCS to reflect the characteristics of brain connectivity, the present study effectively detected the intrinsic brain activity in different frequency bandwidths.

Former studies on intrinsic functional connectivity have focused on the low frequency bands (usually 0.01–0.1 Hz) due to the functional integration of the spontaneous activity of various neuronal processes in low frequencies [74]. Neuroimaging studies have shown that the strength of brain networks is higher in the low frequency band and becomes weaker as the frequency increases [1,55]. The relationship between frequency characteristics of the fMRI signal and its functional implication has been widely explored. For instance, dividing brain BOLD oscillations into four frequency bands, a previous study found opposite visual-motor task-induced shifts between the lowest (0.01–0.05 Hz) and second-to-lowest bands (0.05–0.1 Hz) [75]. In addition, the frequency specificity of regional homogeneity (ReHo) are distinct in different brain regions, such as the frequency band of 0.04–0.1 Hz contributed the most to in the caudate nucleus, and frequencies lower than 0.02 Hz contributed more to ReHo in the putamen [76]. Recently, two frequency bands, 0.01–0.03 Hz and 0.07–0.09 Hz, were demonstrated to contribute primarily to information segregation and integration in functional connectivity [77]. Furthermore, our study demonstrated that the FCS changed the most between the resting states and the mental rotation task states in the low frequency band of 0.05–0.1 Hz rather than in any other bandwidths. All these observations provide evidence that different frequency bands exhibit specific properties in resting and task states, reflecting frequency-dependent functional organizations and implications of intrinsic brain activity.

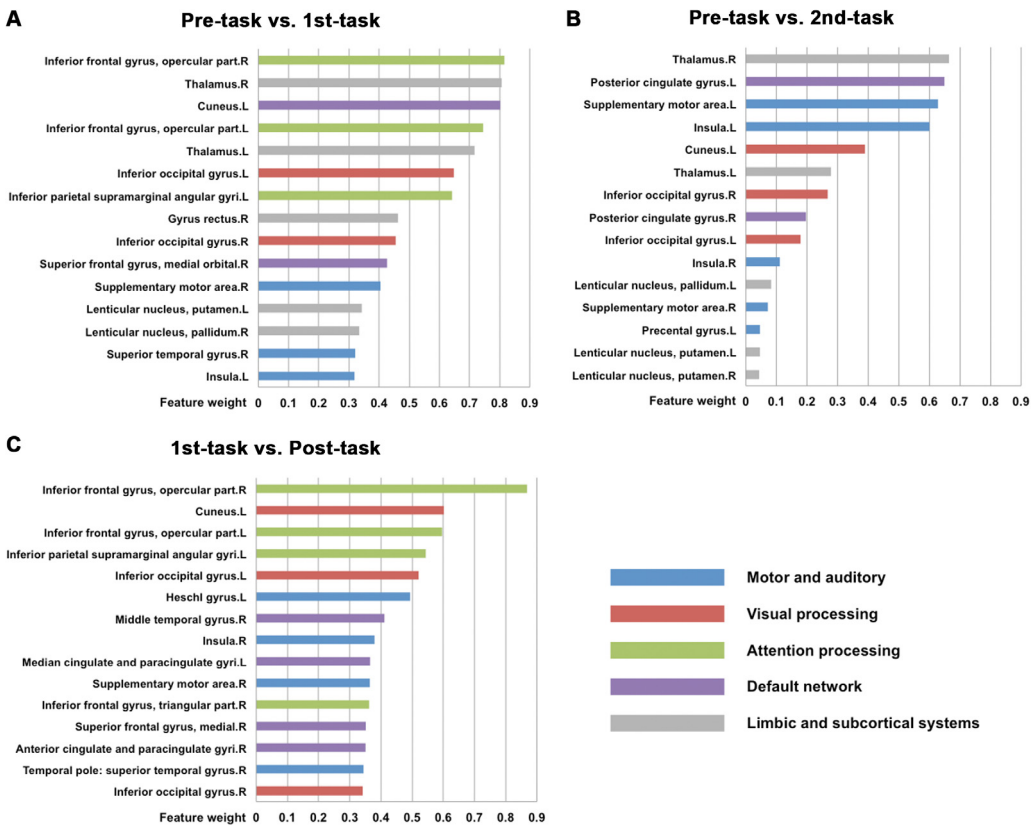

Fig. 7. The discriminative features used for classification among the 3 states. The results of the other states are shown in Fig. S2. All features are listed in descending order of their weights. (A) Discriminative features between pre-task and 1st-task states. (B) Discriminative features between pre-task and 2nd-task states. (C) Discriminative features between 1st-task and post-task states.

In this study, we found that many RSNs are manifested differently in discriminating the resting states and mental rotation task states (Fig. 6), which may have implications for revealing the neural basis of the cognitive processing of mental rotation. First, our data shows that the CEN is the feature that discriminated the most between the mental rotation task state (1st-task state) and resting state (pre-task resting state and post-task resting state). The CEN consists of the dorsolateral prefrontal and posterior parietal cortices and participates in cognitive tasks that require attention [23,78]. Our findings may suggest that the cognitive demand related to attention involvement is the predominate mark of the mental rotation state compared with the resting state, although the participants performed complete practice sessions before the experiment. More importantly, the discriminative mark is not distinct between the 2nd-task state and the resting state. This may show that the adaptive modification of the mental rotation on intrinsic brain activity is dependent on the degree of familiarity with the task. This speculation is also supported by the findings of the DAN, which is an attention resource-related network. It is worth noting that the modulated role of the DAN which contains of superior and inferior parietal regions is different than the CEN. Visual attention often engages in cognitive processes, such as identifying and activating a represented target stimulus and optimizing the external knowledge of the stimulus by shifting attention to its spatial position [79,80]. Activation of the inferior parietal cortex has been identified as a neural correlated performance of mental rotation task [81]. The present study found that the DAN had discriminative power between the 1st-task state and the resting state (pre-task and post-task) but exhibited no significant difference between the 2nd-task state and the pre-task resting state. Similarly, ROIs which participated in attention processing did not have the classification power to discriminate between the 2nd-task state and the pre-task resting state in the validation analysis. Again, we interpreted that, for the 2nd-task state, the subjects had adapted to mental rotation task demand, and the need for attention cognitive resources decreased. This finding is consistent with a mental rotation study in which the mental rotation manipulation influenced the shift of attention and short-term memory encoding [82]. Indeed, many previous studies have shown that the functional reconfiguration of intrinsic brain activity occurred to support the task demands [83–85].

Regarding other aspects, the DMN (aDMN and pDMN) has a relatively high classification power for differentiating the mental rotation task state from the resting state (Fig. 6), which indicates that DMN involvement is a stable feature for distinguishing these states. The validation analysis also showed that brain regions belonging to the DMN, such as the left cuneus, the right middle temporal gyrus, the bilateral posterior cingulate, and the right superior frontal gyrus, have significant classification power (Fig. 7). The DMN is well-known for its role in awake passive states when subjects engage in internally driven cognitive processes, such as self-referential thought, retrieval of past memories, and preparing for the future events [45,86,87]. Our results suggest that the DMN is modulated by mental rotation task, which may further support the idea that mental rotation requires the maintenance of the mentally rotated object in spatial working memory [33]. Notably, the findings of the present study indicate that the CEN and the DMN are both involved in mental rotation manipulation. Studies have found that the SN induces causal control between the CEN and the DMN when engaged in easier decision-making cognitive tasks [88] and that the inter- and causal-connectivities between the SN and

CEN are functionally relevant when engaged in working memory tasks [78]. Correspondingly, the present study also demonstrated that the insula, a core region of the SN, has discriminative power for identifying mental rotation task states from resting states according to the validation analysis, which is consistent with the former findings [33,78,88].

In addition, we noted that the PSMN had a high classification power for discriminating the 1st-/2nd-task states from the pre-task resting state and a relatively high classification power for discriminating the 1st-task state from the post-task resting state (Fig. 6). The results for the 90 ROIs also revealed that the supplementary motor area (SMA) exhibited high classification power (Fig. 7). Mental rotation requires activation of motor-related areas [89], which needs a distinct and distributed brain network, such as the supplementary motor area [8,90]. By comparing the network activities of low and high imagers, researchers had found that the SMA played important roles in computing rotations [90]. In addition, the SMA was found to be involved in implicit motor learning [91]. Along with these findings, our study indicated the PSMN plays an important role in the mental rotation modulation effect on the intrinsic brain activity, which takes part in the cognitive process of rotating objects.

Notably, the PVN, which is an important region for mental imagery processing, has a relatively high classification power for discriminating the mental rotation task states from resting states. The ROIs related to visual processing, such as the inferior occipital gyrus and the cuneus, were also detected the same results (Fig. 7). There is a long-standing question of whether low-level visual features are preserved during mental imagery. The occipital cortex was shown to participate in generating images, which implies the PVN is the neural substrate of mental rotation task in visual imagery and visual perception [92]. Recently, the low-level visual features were found to be encoded in visual mental imagery by constructing voxel-wise encoding models which adjusted to low-level visual features [93]. In addition, a resting-state fMRI study showed that the associated spontaneous activity patterns of the primary visual cortex (i.e., V1) were highly related to visual mental imagery processes during the resting state [94]. Our results, along with the above findings, directly contribute to the view that the low-level PVN is engaged in mental imagery. Furthermore, the involvement of the PVN, PSMN and DMN in the modulatory effect may indicate the importance of mental imagery-based internal mental manipulation in mental rotation task.

In contrast to the apparent discrimination between the mental rotation task state and the resting state, no classification results were found between the pre-task and post-task resting states among the 10 RSNs or the 90 ROIs. Previous studies have reported significant post-task modulation effects on different tasks on intrinsic brain activity, such as an increased connectivity between the left and right middle frontal gyri during the resting period after a language task [95], significant modification of the brain areas involved in the control of spatial attention following a shape-identification task [96], and enhanced functional connectivity between the hippocampus and the lateral occipital complex during resting period after an object-face encoding task with high subsequent memory activation [24]. However, our results of the two resting states closely correspond to a previous report [28] that used small-world configuration to compare the intrinsic brain organizations between among states during a word-picture matching task and found that there was no significant difference in the global and local efficiencies of small-world brain functional networks between pre-task and post-task resting states. These findings may suggest that the observed post-task modulation effects of mental rotation task on intrinsic brain activity predominately embodies the affection of the cognitive executive-control mental components responding to the mental rotation task demands. To support this speculation, the present study demonstrated that the involvement of cognitive executive-control mental components reduced with the familiarity of the task manipulation. Correspondingly, we found that the classification performance between the 2nd-task state and the resting state was lower than that between the 1st-task state and the resting state, and we did not identify any discrimination between the pre-task and post-task resting states. In summary, the present findings show the importance of internal mental manipulation during mental rotation task to a great extent.

Our study focused on the modulation effect of mental rotation on resting states, and reached two primary conclusions. First, we found that the modulated brain regions were highly overlapped with the brain regions activated during mental rotation task in the former studies, which showed that the MLDA could be a useful method to explore the influence of mental rotation on intrinsic brain activity. Second, we detected an important role of the PVN in mental rotation, and the PVN has been demonstrated to be vital for mental imagery. However, previous studies in mental rotation rarely observed the significant function of the PVN in regard to brain regions which responded to mental imagery task [8]. In terms of the modulation effect, the present study showed that the PVN participated in the mental rotation process, which was expected to happen because of the vital role of the PVN in mental imagery. Thereby, exploring the modulatory effect of mental rotation on intrinsic brain activity may provide insight into the neural basis of mental rotation.

There are several issues that remain to be addressed. First, we considered the brain activity which underlies mental rotation task as an integral part, and therefore, this study did not describe specific task-evoked activity patterns. Thus, future studies should implement the canonical hemodynamic response function (HRF) to model the BOLD response during the task state to construct the task network to further explain the task-evoked activity [97]. Second, this study only focused on the "stationary" connectivity of the rest and task states. However, there is a growing trend of studying the time-varying dynamic functional connectivity [98]. Therefore, using a factor analysis of overlapping sliding windows to characterize the task-related dynamic networks in future work will provide new insight into the current research topic. Finally, the individual patterns of brain connectivity were not taken into consideration in the current study. Thus, future studies should focus on individual variability to explore the neural mechanisms of mental rotation [98,99].

5. Conclusion

In summary, the present study adopted the MLDA method to investigate the FCS modulatory effect of mental rotation on intrinsic brain activity over four brain states. We found that the FCS of spontaneous brain activity in a specific low frequency bandwidth of 0.05–0.1 Hz could effectively discriminate the mental rotation task state from the resting state, in which the cognitive executive-control network (i.e., CEN, DAN, and SN) and the imagery-based internal mental manipulation network (DMN, PSMN, and PVN) played important roles. Imagery manipulation was a consistent element in the mental rotation, while the involvement of executive-control was dependent on the degree of familiarity of the task. Regarding the relation between mental rotation and intrinsic brain activity, the present work showed the importance of the imagery-based mental manipulation which underlies cognitive executive-control function during mental rotation task, which provides further insight into the neural mechanisms of mental rotation.

Competing interest statement

The authors declare that they have no competing financial interests

Acknowledgements

This work was supported by the Natural Science Foundation of China (No. 31371049), the Guangdong Provincial Natural Science Foundation of China (No. 2014A030310487), and the School of Psychology of South China Normal University (No. hsxly2016021).

Appendix A. Supplementary data

Supplementary data associated with this article can be found, in the online version, at http://dx.doi.org/10.1016/j.bbr.2016.12.017.

References

[1] X. Li, E.G. Kehoe, T.M. McGinnity, D. Coyle, A.L.W. Bokde, Modulation of effective connectivity in the default mode network at rest and during a memory task, Brain Connect 5 (1) (2015) 60–67.
[2] D.M.E. Torta, Parcellation of the cingulate cortex at rest and during tasks: a meta-analytic clustering and experimental study, Front. Hum. Neurosci. 7 (9) (2013) 275.
[3] M.E. Raichle, A.M. MacLeod, A.Z. Snyder, W.J. Powers, D.A. Gusnard, G.L. Shulman, A default mode of brain function, Proc. Natl. Acad. Sci. U. S. A. 98 (2) (2001) 676–682.
[4] A. Fornito, B.J. Harrison, A. Zalesky, J.S. Simons, Competitive and cooperative dynamics of large-scale brain functional networks supporting recollection, Proc. Natl. Acad. Sci. U. S. A. 109 (31) (2012) 12788–12793.
[5] W. Gao, W. Lin, Frontal parietal control network regulates the anti-correlated default and dorsal attention networks, Hum. Brain Mapp. 33 (1) (2012) 192–202.
[6] R.N. Shepard, J. Metzler, Mental rotation of three-dimensional objects, Science 171 (3972) (1971) 701–703.
[7] A. Gogos, M. Gavrilescu, S. Davison, K. Searle, J. Adams, S.L. Rossell, R. Bell, S.R. Davis, G.F. Egan, Greater superior than inferior parietal lobule activation with increasing rotation angle during mental rotation: an fMRI study, Neuropsychologia 48 (2) (2010) 529–535.
[8] J. Zacks, Neuroimaging studies of mental rotation: a meta-analysis and review, J. Cognit. Neurosci. 20 (1) (2008) 1–19.
[9] L.M. Wierenga, M.P.V.D. Heuvel, S.V. Dijk, Y. Rijks, M.A.D. Reus, S. Durston, The development of brain network architecture, Hum. Brain Mapp. 37 (2) (2016) 717–729.
[10] N.A. Crossley, P.T. Fox, E.T. Bullmore, Meta-connectomics: human brain network and connectivity meta-analyses, Psychol. Med. 46 (5) (2016) 1–11.
[11] Z. Zhang, W. Liao, H. Chen, D. Mantini, J.R. Ding, Q. Xu, Z. Wang, C. Yuan, G. Chen, Q. Jiao, Altered functional-structural coupling of large-scale brain networks in idiopathic generalized epilepsy, Brain 134 (Pt. 10) (2011) 2912–2928.
[12] C.H. Zhang, Y. Lu, B. Brinkmann, K. Welker, G. Worrell, B. He, Lateralization and localization of epilepsy related hemodynamic foci using presurgical fMRI, Clin. Neurophysiol. 126 (1) (2015) 27–38.
[13] M. Bola, C. Gall, B.A. Sabel, Disturbed temporal dynamics of brain synchronization in vision loss, Cortex 67 (2015) 134–146.
[14] M.M. Bohlken, R.M. Brouwer, R.C.W. Mandl, A.M. Hedman, M.P.V.D. Heuvel, N.E.M.V. Haren, R.S. Kahn, H.E.H. Pol, Topology of genetic associations between regional gray matter volume and intellectual ability: evidence for a high capacity network, Neuroimage 124 (Pt A) (2016) 1044–1053.
[15] W. Yang, L. Cun, X. Du, J. Yang, Y. Wang, D. Wei, Q. Zhang, Q. Jiang, Gender differences in brain structure and resting-state functional connectivity related to narcissistic personality, Sci. Rep. 5 (2015) 1–12.
[16] G.G. Knyazev, N.V. Volf, L.V. Belousova, Age-related differences in electroencephalogram connectivity and network topology, Neurobiol. Aging 36 (5) (2015) 1849–1859.
[17] A.C. Hill, A.R. Laird, J.L. Robinson, Gender differences in working memory networks: a BrainMap meta-analysis, Biol. Psychol. 102 (5) (2014) 18–29.
[18] V.D. Calhoun, K.A. Kiehl, G.D. Pearlson, Modulation of temporally coherent brain networks estimated using ICA at rest and during cognitive tasks, Hum. Brain Mapp. 29 (7) (2008) 828–838.
[19] M. Bianciardi, M. Fukunaga, P.V. Gelderen, S.G. Horovitz, J.A.D. Zwart, J.H. Duyn, Modulation of spontaneous fMRI activity in human visual cortex by behavioral state, NeuroImage 45 (1) (2008) 160–168.
[20] V.J. Kiviniemi, H. Haanpää, J.H. Kantola, J. Jauhiainen, V. Vainionpää, S. Alahuhta, O. Tervonen, Midazolam sedation increases fluctuation and synchrony of the resting brain BOLD signal, Magn. Reson. Imaging 23 (4) (2005) 531–537.
[21] M.J. Lowe, B.J. Mock, J.A. Sorenson, Functional connectivity in single and multislice echoplanar imaging using resting-state fluctuations, NeuroImage 7 (2) (1998) 119–132.
[22] D. Cordes, V.M. Haughton, K. Arfanakis, J.D. Carew, P.A. Turski, C.H. Moritz, M.A. Quigley, M.E. Meyerand, Frequencies contributing to functional connectivity in the cerebral cortex in resting-state data, AJNR Am. J. Neuroradiol. 22 (7) (2001) 1326–1333.
[23] M.D. Fox, M. Corbetta, A.Z. Snyder, J.L. Vincent, M.E. Raichle, Spontaneous neuronal activity distinguishes human dorsal and ventral attention systems, Proc. Natl. Acad. Sci. U. S. A. 103 (36) (2006), 13560–13560.
[24] A. Tambini, N. Ketz, L. Davachi, Enhanced brain correlations during rest are related to memory for recent experiences, Neuron 65 (2) (2010) 280–290.
[25] N.B. Albert, E.M. Robertson, R.C. Miall, The resting human brain and motor learning, Curr. Biol. 19 (12) (2009) 1023–1027.
[26] A. Elton, G. Wei, Task-related modulation of functional connectivity variability and its behavioral correlations, Hum. Brain Mapp. 36 (2015) 3260–3272.
[27] K.C. Tung, J. Uh, D. Mao, F. Xu, G. Xiao, H. Lu, Alterations in resting functional connectivity due to recent motor task, NeuroImage 78 (2013) 316–324.
[28] Z. Wang, J. Liu, N. Zhong, Y. Qin, H. Zhou, K. Li, Changes in the brain intrinsic organization in both on-task state and post-task resting state, NeuroImage 62 (1) (2012) 394–407.
[29] P.A. Howardjones, T. Jay, A. Mason, H. Jones, Gamification of learning deactivates the default mode network, Front. Psychol. 6 (e9251) (2016) 1891.
[30] Y. Hu, X. Chen, H. Gu, Y. Yang, Resting-state glutamate and GABA concentrations predict task-induced deactivation in the default mode network, J. Neurosci. 33 (47) (2013) 18566–18573.
[31] C.L. Grady, A.B. Protzner, N. Kovacevic, S.C. Strother, B. Afshinpour, M. Wojtowicz, J.A. Anderson, N. Churchill, A.R. Mcintosh, A multivariate analysis of age-related differences in default mode and task-positive networks across multiple cognitive domains, Cereb. Cortex 20 (6) (2010) 1432–1447.
[32] A. Anticevic, G. Repovs, G.L. Shulman, D.M. Barch, When less is more: TPJ and default network deactivation during encoding predicts working memory performance, NeuroImage 49 (3) (2010) 2638–2648.
[33] J.R. Booth, B. MacWhinney, K.R. Thulborn, K. Sacco, J.T. Voyvodic, H.M. Feldman, Developmental and lesion effects in brain activation during sentence comprehension and mental rotation, Dev. Neuropsychol. 18 (2) (2000) 139–169.
[34] M. Dalecki, S. Dern, F. Steinberg, Mental rotation of a letter, hand and complex scene in microgravity, Neurosci. Lett. 533 (2013) 55–59.
[35] M. Thomas, M. Dalecki, V. Abeln, EEG coherence during mental rotation of letters, hands and scenes, Int. J. Psychophysiol. 89 (1) (2013) 128–135.
[36] M.S. Cohen, S.Y. Bookheimer, Localization of brain function using magnetic resonance imaging, Trends Neurosci. 17 (7) (1994) 268–277.
[37] I.M. Harris, G.F. Egan, C. Sonkkila, H.J. Tochondanguy, G. Paxinos, J.D.G. Watson, Selective right parietal lobe activation during mental rotation: a parametric PET study, Brain 123 (Pt. 1) (2000) 65–73.
[38] H. Koshino, P.A. Carpenter, T.A. Keller, M.A. Just, Interactions between the dorsal and the ventral pathways in mental rotation: an fMRI study, Cogn. Affect Behav. Neurosci. 5 (1) (2005) 54–66.
[39] K. Podzebenko, G.F. Egan, J.D. Watson, Real and imaginary rotary motion processing: functional parcellation of the human parietal lobe revealed by fMRI, J. Cognit. Neurosci. 17 (1) (2005) 24–36.
[40] C. Ecker, M. Brammer, S. Williams, Combining path analysis with time-resolved functional magnetic resonance imaging: the neurocognitive network underlying mental rotation, J. Cognit. Neurosci. 20 (6) (2008) 1003–1020.
[41] P.A. Carpenter, M.A. Just, T.A. Keller, W. Eddy, K. Thulborn, Graded functional activation in the visuospatial system with the amount of task demand, J. Cognit. Neurosci. 11 (1) (1999) 9–24.
[42] K. Podzebenko, G. Egan, J. Watson, Real and imaginary rotary motion processing: functional parcellation of the human parietal lobe revealed by fMRI, J. Cognit. Neurosci. 17 (1) (2005) 24–36.
[43] E.C. Leek, S.J. Johnston, Correspondence functional specialization in the supplementary motor complex, Nat. Rev. Neurosci. 10 (1) (2009) 78.
[44] X. Liang, Q. Zou, Y. He, Y. Yang, Coupling of functional connectivity and regional cerebral blood flow reveals a physiological basis for network hubs of the human brain, Proc. Natl. Acad. Sci. U. S. A. 110 (5) (2013) 1929–1934.
[45] R.L. Buckner, J. Sepulcre, T. Talukdar, F.M. Krienen, H. Liu, T. Hedden, J.R. Andrews-Hanna, R.A. Sperling, K.A. Johnson, Cortical hubs revealed by intrinsic functional connectivity: mapping, assessment of stability, and relation to Alzheimer's disease, J. Neurosci. 29 (6) (2009) 1860–1873.
[46] B.-K. Yuan, J. Wang, Y.-F. Zang, D.-Q. Liu, Amplitude differences in high-frequency fMRI signals between eyes open and eyes closed resting states, Front. Hum. Neurosci. 8 (2014) 503.
[47] J.R. Sato, A. Fuita, C.E. Thomaz, M.d.G. Morais Martin, J. Mourao-Miranda, M.J. Brammer, E. Amaro Junior, Evaluating SVM and MLDA in the extraction of discriminant regions for mental state prediction, NeuroImage 47 (1) (2009) 423–425.
[48] T. Kasparek, C.E. Thomaz, J.R. Sato, D. Schwarz, E. Janousova, R. Marecek, R. Prikryl, J. Vanicek, A. Fujita, E. Ceskova, Maximum-uncertainty linear discrimination analysis of first-episode schizophrenia subjects, Psychiatry Res. 191 (3) (2011) 174–181.
[49] Z. Dai, C. Yan, Z. Wang, J. Wang, M. Xia, K. Li, Y. He, Discriminative analysis of early Alzheimer's disease using multi-modal imaging and multi-level characterization with multi-classifier (M3), NeuroImage 59 (3) (2012) 2187–2195.

[50] N. Tzourio-Mazoyer, B. Landeau, D. Papathanassiou, F. Crivello, O. Etard, N. Delcroix, B. Mazoyer, M. Joliot, Automated anatomical labeling of activations in SPM using a macroscopic anatomical parcellation of the MNI MRI single-subject brain, NeuroImage 15 (1) (2002) 273–289.
[51] P. Shah, A. Miyake, The separability of working memory resources for spatial thinking and language processing: an individual differences approach, Q. J. Exp. Psychol.—Gen. 125 (1) (1996) 4–27.
[52] P.J. Rousseeuw, C. Croux, Alternatives to the median absolute deviation, J. Am. Stat. Assoc. 88 (424) (1993) 1273–1283.
[53] A. Meyler, T.A. Keller, V.L. Cherkassky, D. Lee, F. Hoeft, S. Whitfield-Gabrieli, J.D. Gabrieli, M.A. Just, Brain activation during sentence comprehension among good and poor readers, Cereb. Cortex 17 (12) (2007) 2780–2787.
[54] J. Ashburner, K.J. Friston, Unified segmentation, NeuroImage 26 (3) (2005) 839–851.
[55] L. Wang, M. Xia, K. Li, Y. Zeng, Y. Su, W. Dai, Q. Zhang, Z. Jin, P.B. Mitchell, X. Yu, The effects of antidepressant treatment on resting-state functional brain networks in patients with major depressive disorder, Hum. Brain Mapp. 36 (2) (2015) 768–778.
[56] R.L. Carhart-Harris, K.J. Friston, The default-mode, ego-functions and free-energy: a neurobiological account of Freudian ideas, Brain 133 (2010) 1265–1283.
[57] V.D. Calhoun, T. Adali, G.D. Pearlson, J.J. Pekar, A method for making group inferences from functional MRI data using independent component analysis, Hum. Brain Mapp. 14 (3) (2001) 140–151.
[58] A.J. Bell, T.J. Sejnowski, An information maximization approach to blind sepatation and blind deconvolution, Neural Comput. 7 (6) (1995) 1129–1159.
[59] J. Himberg, A. Hyvarinen, F. Esposito, Validating the independent components of neuroimaging time series via clustering and visualization, NeuroImage 22 (3) (2004) 1214–1222.
[60] S.A. Meda, M.C. Stevens, B.S. Folley, V.D. Calhoun, G.D. Pearlson, Evidence for anomalous network connectivity during working memory encoding in schizophrenia: an ICA based analysis, PLoS One 4 (11) (2009) e7911.
[61] J.R. Chumbley, K.J. Friston, False discovery rate revisited: FDR and topological inference using Gaussian random fields, NeuroImage 44 (1) (2009) 62–70.
[62] C.E. Thomaz, E.C. Kitani, D.F. Gillies, A maximum uncertainty LDA-based approach for limited sample size problems—with application to face recognition, J. Braz. Comput. Soc. 12 (2) (2006) 7–18.
[63] L. Wei, D. Mantini, Z. Zhang, Z. Pan, J. Ding, Q. Gong, Y. Yang, H. Chen, Evaluating the effective connectivity of resting state networks using conditional Granger causality, Biol. Cybern. 102 (1) (2010) 57–69.
[64] K. Jann, M. Kottlow, T. Dierks, C. Boesch, T. Koenig, Topographic electrophysiological signatures of fMRI resting state networks, PLoS One 5 (9) (2010), 494–494.
[65] R. Li, K. Chen, A.S. Fleisher, E.M. Reiman, L. Yao, X. Wu, Large-scale directional connections among multi resting-state neural networks in human brain: a functional MRI and Bayesian network modeling study, NeuroImage 56 (3) (2011) 1035–1042.
[66] J.S. Damoiseaux, S.A.R.B. Rombouts, F. Barkhof, P. Scheltens, C.J. Stam, S.M. Smith, C.F. Beckmann, Consistent resting-state networks across healthy subjects, Proc. Natl. Acad. Sci. U. S. A. 103 (37) (2006) 13848–13853.
[67] D. Sridharan, D.J. Levitin, V. Menon, A critical role for the right fronto-insular cortex in switching between central-executive and default-mode networks, Proc. Natl. Acad. Sci. U. S. A. 105 (34) (2008) 12569–12574.
[68] Y. He, J. Wang, L. Wang, Z.J. Chen, C. Yan, H. Yang, H. Tang, C. Zhu, Q. Gong, Y. Zang, Uncovering intrinsic modular organization of spontaneous brain activity in humans, PLoS One 4 (4) (2009) e5226.
[69] M. Muehlhan, C. Kirschbaum, H.U. Wittchen, N. Alexander, Epigenetic variation in the serotonin transporter gene predicts resting state functional connectivity strength within the salience-network, Hum. Brain Mapp. 36 (11) (2015) 4361–4371.
[70] S. Ray, S.R. Gohel, B.B. Biswal, Altered functional connectivity strength in abstinent chronic cocaine smokers compared to healthy controls, Brain Connect 5 (8) (2015) 476–486.
[71] Q. Su, D. Yao, M. Jiang, F. Liu, J. Jiang, C. Xu, Y. Dai, M. Yu, L. Long, H. Li, Increased functional connectivity strength of right inferior temporal gyrus in first-episode, drug-naive somatization disorder, Aust. N. Z. J. Psychiatry 49 (1) (2015) 74–81.
[72] L. Pan, Y. Yong, J. Jovicich, N.D. Pisapia, W. Xiang, C.S. Zuo, J.J. Levitt, Static and dynamic posterior cingulate cortex nodal topology of default mode network predicts attention task performance, Brain Imaging Behav. 10 (1) (2015) 1–14.
[73] W. Zhang, L. Hong, X. Pan, Positive and negative affective processing exhibit dissociable functional hubs during the viewing of affective pictures, Hum. Brain Mapp. 36 (2) (2014) 415–426.
[74] S.R. Gohel, B.B. Biswal, Functional integration between brain regions at rest occurs in multiple-frequency bands, Brain Connect 5 (1) (2014) 23–24.
[75] A.T. Baria, M.N. Baliki, T. Parrish, A.V. Apkarian, Anatomical and functional assemblies of brain BOLD oscillations, J. Neurosci. 31 (21) (2011) 7910–7919.
[76] X. Song, Y. Zhang, Y. Liu, Frequency specificity of regional homogeneity in the resting-state human brain, PLoS One 9 (1) (2014) e86818.
[77] S. Sasai, F. Homae, H. Watanabe, A.T. Sasaki, H.C. Tanabe, N. Sadato, G. Taga, Frequency-specific network topologies in the resting human brain, Front. Hum. Neurosci. 8 (2014) 1022.
[78] X. Fang, Y. Zhang, Y. Zhou, L. Cheng, J. Li, Y. Wang, K.J. Friston, T. Jiang, Resting-state coupling between core regions within the central-executive and salience networks contributes to working memory performance, Front. Behav. Neurosci. 10 (27) (2016) 1–11.
[79] B. Brisson, P. Jolicoeur, A psychological refractory period in access to visual short-term memory and the deployment of visual-spatial attention: multitasking processing deficits revealed by event-related potentials, Psychophysiology 44 (2) (2007) 323–333.
[80] B. Brisson, P. Jolicoeur, Electrophysiological evidence of central interference in the control of visuospatial attention, Psychon. Bull. Rev. 14 (1) (2007) 126–132.
[81] C. Hoppe, K. Fliessbach, S. Stausberg, J. Stojanovic, P. Trautner, C.E. Elger, B. Weber, A key role for experimental task performance: effects of math talent, gender and performance on the neural correlates of mental rotation, Brain Cogn. 78 (1) (2012) 14–27.
[82] M.M. Pannebakker, P. Jolicoeur, W.O. van Dam, G.P.H. Band, K.R. Ridderinkhof, B. Hommel, Mental rotation impairs attention shifting and short-term memory encoding: neurophysiological evidence against the response-selection bottleneck model of dual-task performance, Neuropsychologia 49 (11) (2011) 2985–2993.
[83] D.S. Bassett, N.F. Wymbs, M.A. Porter, P.J. Mucha, J.M. Carlson, S.T. Grafton, Dynamic reconfiguration of human brain networks during learning, Proc. Natl. Acad. Sci. U. S. A. 108 (18) (2011) 7641–7646.
[84] M. Bola, B.A. Sabel, Dynamic reorganization of brain functional networks during cognition, NeuroImage 114 (2015) 398–413.
[85] D. Vatansever, D.K. Menon, A.E. Manktelow, B.J. Sahakian, E.A. Stamatakis, Default mode network connectivity during task execution, NeuroImage 122 (2015) 96–104.
[86] R.N. Spreng, R.A. Mar, A.S.N. Kim, The common neural basis of autobiographical memory, prospection, aavigation, theory of mind, and the default mode: a auantitative meta-analysis, J. Cognit. Neurosci. 21 (3) (2009) 489–510.
[87] B. Hahn, T.J. Ross, E.A. Stein, Cingulate activation increases dynamically with response speed under stimulus unpredictability, Cereb. Cortex 17 (7) (2007) 1664–1671.
[88] G.B. Chand, M. Dhamala, Interactions among the brain default-mode, salience, and central-executive networks during perceptual decision-making of moving dots, Brain Connect 6 (3) (2016) 249–254.
[89] E.C. Leek, K.S.L. Yuen, S.J. Johnston, Domain general sequence operations contribute to pre-SMA involvement in visuo-spatial processing, Front. Hum. Neurosci. 10 (2016) 9.
[90] R.H. Logie, C.R. Pernet, A. Buonocore, S. Della Sala, Low and high imagers activate networks differentially in mental rotation, Neuropsychologia 49 (11) (2011) 3071–3077.
[91] Y.K. Kim, S.H. Shin, Comparison of effects of transcranial magnetic stimulation on primary motor cortex and supplementary motor area in motor skill learning (randomized, cross over study), Front. Hum. Neurosci. 8 (2014) 937.
[92] D.G. Pearson, C. Deeprose, S.M.A. Wallace-Hadrill, S.B. Heyes, E.A. Holmes, Assessing mental imagery in clinical psychology: a review of imagery measures and a guiding framework, Clin. Psychol. Rev. 33 (1) (2013) 1–23.
[93] T. Naselaris, C.A. Olman, D.E. Stansbury, K. Ugurbil, J.L. Gallant, A voxel-wise encoding model for early visual areas decodes mental images of remembered scenes, NeuroImage 105 (2014) 215–228.
[94] K. Wang, T. Jiang, C. Yu, L. Tian, J. Li, Y. Liu, Y. Zhou, L. Xu, M. Song, K. Li, Spontaneous activity associated with primary visual cortex: a resting-state FMRI study, Cereb. Cortex 18 (3) (2008) 697–704.
[95] A.B. Waites, A. Stanislavsky, D.F. Abbott, G.D. Jackson, Effect of prior cognitive state on resting state networks measured with functional connectivity, J. Exp. Biol. 24 (1) (2005) 4309–4315.
[96] C.M. Lewis, A. Baldassarre, G. Committeri, G.L. Romani, M. Corbetta, Learning sculpts the spontaneous activity of the resting human brain, Proc. Natl. Acad. Sci. U. S. A. 106 (41) (2009) 17558–17563.
[97] J. Rissman, A. Gazzaley, M. D'Esposito, Measuring functional connectivity during distinct stages of a cognitive task, NeuroImage 23 (2) (2004) 752–763.
[98] T.M. Madhyastha, M.K. Askren, P. Boord, T.J. Grabowski, Dynamic connectivity at rest predicts attention task performance, Brain Connect 5 (1) (2015) 45–59.
[99] I. Tavor, J.O. Parker, R.B. Mars, S.M. Smith, T.E. Behrens, S. Jbabdi, Task-free MRI predicts individual differences in brain activity during task performance, Science 352 (6282) (2016) 216–220.